Eur. Phys. J. B **61**, 165–171 (2008)
DOI: 10.1140/epjb/e2008-00064-6

THE EUROPEAN PHYSICAL JOURNAL B

Structural, electronic and optical properties of $SrCl_2$ under hydrostatic stress

Y. Benmimoun[1], A. Bouhemadou[2,a], R. Khenata[1,b], A.H. Reshak[3], B. Amrani[1], M. Ameri[4], and H. Baltache[1]

[1] Institute of Science and Technology, University of Mascara, 29000 Mascara, Algeria
[2] Department of Physics, Faculty of Science, University of Setif, 19000 Setif, Algeria
[3] Institute of Physical Biology, University of S. Bohemia, Institute of System Biology and Ecology Academy of Sciences, Nove Hrady 373 33, Czech Republic
[4] Department of Physics, Faculty of Science, University Djilali Liabès, 22000 Sid-Bel-Abbès, Algeria

Received 1st September 2007 / Received in final form 21 December 2007
Published online 16 February 2008 –

Abstract. The results of first-principles theoretical study of the structural, electronic and optical properties of $SrCl_2$ in its cubic structure, have been performed using the full-potential linear augmented plane-wave method plus local orbitals (FP-APW+lo) as implemented in the WIEN2k code. In this approach both the local density approximation (LDA) and the generalized gradient approximation (GGA) are used for the exchange-correlation (XC) potential. Also we have used the Engel-Vosko GGA formalism, which optimizes the corresponding potential for band structure calculations. We performed these calculations with and without spin-orbit interactions. Including spin-orbit coupling cause to lifts the triple degeneracy at Γ point and a double degeneracy at X point. Results are given for structural properties. The pressure dependence of elastic constants and band gaps are investigated. The dielectric function, reflectivity spectra and refractive index are calculated up to 30 eV. Also we calculated the pressure and volume dependence of the static optical dielectric constant.

PACS. 71.15.Ap Basis sets (LCAO, plane-wave, APW, etc.) and related methodology (scattering methods, ASA, linearized methods, etc.) – 78.40.Fy Semiconductors – 78.20.Ci Optical constants (including refractive index, complex dielectric constant, absorption, reflection and transmission coefficients, emissivity)

1 Introduction

The study of pressure dependence of band gaps of materials is of fundamental interest because insight into the electronic and optical properties of strained super lattice can be gained by understanding of effect of strain on bulk simples of materials [1], also interest in this area arose results of the development of diamond- anvil cell and the ruby fluorescence manometer. Over the years, the pressure coefficients of band gaps in materials have been widely studied using varying techniques [2–4].

The structure of the AX_2 compounds can be divided into four main groups based on the constituent cation-centered anion polyhedra: the quartz group, the rutile group, the fluorite group and the conmnite group, in which the coordination number is four (tetrahedra), six (octahedra), eight (cube) and nine (elongated tricapped trigonal prism), respectively [5]. The fluorite group or (CaF_2-type) structure have eight fluorine atoms arranged in a cube around the calcium atoms, with the cubes of fluorine edge-connected in a face-centered cubic array. Conversely, the fluorine atom is surrounded by four calcium atoms arranged in an ideal tetrahedron, with the tetrahedral also edge-connected [6].

Compounds which have the fluorite structure; e.g. CaF_2, SrF_2, BaF_2, $SrCl_2$ and PbF_2, exhibit fast-ions conduction at high temperature [7,8] and they have attracted considerable attentions due to their technological applications in solid state electrolyte, in fuel cell or solid state gas-detectors. A chemical reaction between strontium chloride and CO_2 product materials which found application in plastic and medicine areas [9]. Also by their other remarkable and interesting physical properties. There is a considerable theoretical and experimental work involving structural, elastic, and optical properties under ambient and high pressure for CaF_2, SrF_2, BaF_2 compounds [10–12]. There are many studies [13–21] has been reported on $SrCl_2$ compounds. In particular the structural phase transitions of $SrCl_2$ have been studied by Brixner [13]. The ionic conductivity studies at high temperature have been performed by Voronin and Volkov [14]. Jennison and

[a] e-mail: a_bouhemadou@yahoo.fr
[b] e-mail: khenata_rabah@yahoo.fr

Kunz [15] have used the Hartree-Fock method to calculate the charge density profile of $SrCl_2$. Excited states, emission spectra and luminescence properties have been investigated experimentally by several authors [16–19]. The elastic constants of $SrCl_2$ crystal have been determined using the ultrasonic pulse eco-technique more than forty years ago by Lauer and co-authors [20]. Recently Kanchana et al. [21] have been used the full potential linear muffin tin-orbital (FP-LMTO) method to investigate the electronic structure of $SrCl_2$ compound with emphasis on the ground state and elastic properties.

From the above it is clear that although there is considerable work involving both experimental and theoretical methods on $SrCl_2$ compound. There are very few theoretical studies on structural, electronic and elastic properties are reported. To the best of our knowledge, there are no earlier theoretical calculations for the optical properties and the pressure dependence of band gaps and elastic constants that have been reported for this compound. We therefore think it is worthwhile to perform these calculations using the full-potential linear augmented plane-wave method plus local orbitals (FP-APW+lo) method which has proven to be one of the most accurate methods [22,23] for the computation of the electronic structure of solids within density functional theory (DFT) in order to complete the exciting experimental and theoretical work for this compound.

2 Computational method

$SrCl_2$ compound have the (CaF_2-type) structure. The Sr atom is located at (0; 0; 0) and the Cl atoms at (0.25; 0.25; 0.25) and (0.75; 0.75; 0.75). The lattice constant $a$is 6.9744 Å [24]. The calculations reported here were carried out by means of the FP-APW+lo method [25,26] using WIEN2K computer package [27]. We performed these calculations with and without spin-orbit interactions. The spin orbit coupling in our calculations performed by using the second variation method programmed in the WIEN2K code. The exchange correlation (XC) effects for the structural properties are treated by the local density approximation (LDA) [28] with and without generalized gradient approximation (GGA) [29]. It is well-known both LDA and GGA usually underestimate the energy gap [31]. For this reason we used the Engel and Vosko scheme (EV-GGA) [30] to calculate the electronic and optical properties.

In order to achieve energy eigenvalues convergence, the wave functions in the interstitial region were expanded in plane waves with a cut-off $K_{max} = 9/R_{\mathrm{MT}}$, where R_{MT} denotes the smallest atomic sphere radius and K_{max} gives the magnitude of the largest K vector in the plane wave expansion. The R_{MT} are taken to be 2.5 and 2.3 atomic units (a.u.) for Sr and Cl, respectively. The valence wave functions in side the spheres are expanded up to $l_{max} = 10$ while the charge density was Fourier expanded up to $G_{max} = 14$. The self-consistent calculations are considered to be converged when the total energy of the system is stable within 10^{-4} Ry. The integrals over the Brillouin zone are performed up to 18 $\boldsymbol{k}$-points in the irreducible Brillouin zone (IBZ), using the Monkhorst-Pack special $\boldsymbol{k}$-points approach [32].

Table 1. Calculated lattice constant a_0 (in Å), bulk modulus B_0 (in GPa), pressure derivative B' and elastic constants C_{ij} (in GPa) for $SrCl_2$ at equilibrium volume compared to the experimental data and other work.

	Present work		Experimental	Theoretical[c]
	LDA	GGA		GGA- LMTO
a(Å)	6.801	7.042	6.9744[a]	7.032
B_0(GPa)	44.5	37.2	34.3[b]	35.3
B'	4.31	3.38		
C_{11}	82.3	70.5	70.2[b]	66.9
C_{12}	25.6	20.5	17.3[b]	19.6
C_{44}	27.2	14.2	9.72[b]	9.9
E	68.7	47.6	40.3[b]	42.9
Y	27.6	18.5	16.6[b]	15.4
ζ	0.4	0.4		

[a]Reference [24]; [b] reference [20]; [c] reference [21].

3 Results and discussions

3.1 Structural and elastic properties

The fitting of the Murnaghan equation of state [33] to the total energies versus lattice parameters, yields to the equilibrium lattice parameter (a_0), bulk modulus B_0, and the pressure derivative of the bulk modulus B'. In Table 1, we summarize our calculated structural properties (lattice constant, bulk modulus and its pressure derivative) of $SrCl_2$ at ambient pressure. When we analyze our results we found that there is good agreement between our results and the previous theoretical calculations. In comparison with the experimental data we found that GGA overestimate the lattice parameter. While LDA underestimate them, which are consistent with the general trend of these approximations [34,35]. To verify the accuracy of these results, several tests have been performed using different muffin-tin radius as well as different sets of special $\boldsymbol{k}$-point to ensure the convergence.

The elastic properties play an important role in providing valuable information about the binding characteristic between adjacent atomic planes. Anisotropic characters of binding and structural stability are usually defined by the elastic constants C_{ij}. These constants have been often related to the shear modulus G and Young's modulus Y, which are frequently measured for polycrystalline materials when investigating their hardness. The elastic moduli require knowledge of the derivative of the energy as a function of the lattice strain. In the case of cubic system, this strain is chosen in such a way that the volume of the unit cell is preserved. Thus for the calculation of elastic constants C_{11}, C_{12} and C_{44} for this compound we used the method discussed in detail in reference [36], and applied successfully in our previous works [37,38] and Sahara et al. [39]. On the other hand, the shear and the Young's

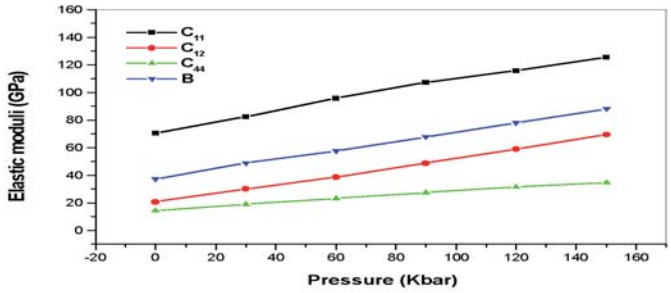

Fig. 1. Pressure dependence of C_{ij} and B_0 for $SrCl_2$ with GGA.

moduli are related to the microscopic elastic constants by means of the following equations:

$$G = 9BY/(3B + Y) \text{ and } Y = (C_{11} - C_{12} + 3C_{44})/5. \quad (1)$$

Another important parameter is the internal strain parameter introduced by Kleinman [40] and describes the relative positions of the cation and anion sublattices under volume, conserving strain distortions for which positions are not fixed by symmetry. We use the following relation [41,42]:

$$\zeta = \frac{C_{11} + 8C_{12}}{7C_{11} + 2C_{12}}. \quad (2)$$

The calculated elastic constantsC_{ij}, the shear and the Young's modulus and the internal parameter ζ are summarized in Table 1 together with the available experimental data and results of previous calculations. When we analyze the results of the elastic constants we can state that the GGA gave comparatively higher lattice parameter and smaller bulk modulus than the LDA. Hence, the calculated GGA-elastic constants by using the known relation $B = (C_{11} + 2C_{12})/3$ are relatively small compared to those of LDA. We worth noting that the relaxation has a strong effects on the elastic constants, especially for C_{44} which is most sensitive to the relaxation of the positions of anionic atoms in the [001] direction [43,44], thus we state that the slight differences between our calculated elastic constants and that reported in reference [21] is a consequence of not re-optimizing of the chlorine positions. However, our results are in reasonable agreement with the experiment results and other calculations.

The requirement of mechanical stability in this cubic structure leads to the following restrictions on the elastic constants, $C_{11} - C_{12} > 0$, $C_{44} > 0$, $C_{11} + 2C_{12} > 0$ and $C_{12} < B < C_{11}$, indicating that this compound is stable against elastic deformations.

Now we are interested to study the pressure dependence of the elastic properties. In Figure 1, we present the variation of elastic constants and bulk modulus of $SrCl_2$ with respect to the variation of pressure. We clearly observed a linear dependence in all curves in the considered range of pressure. In Table 2, we listed our results for the pressure derivatives $\partial B_0/\partial P$, $\partial C_{11}/\partial P$, $\partial C_{12}/\partial P$ and $\partial C_{44}/\partial P$ for both LDA and GGA. We notice that the elastic constants C_{11}, C_{12}, C_{44} and bulk modulus increases

Table 2. Calculated pressure derivatives of the elastic moduli for cubic $SrCl_2$ compound.

	$\frac{\partial B_0}{\partial P}$	$\frac{\partial C_{11}}{\partial P}$	$\frac{\partial C_{12}}{\partial P}$	$\frac{\partial C_{44}}{\partial P}$
FP-LAPW-GGA	3.35	3.60	3.25	1.37
FP-LAPW-LDA	4.31	4.25	3.49	0.43

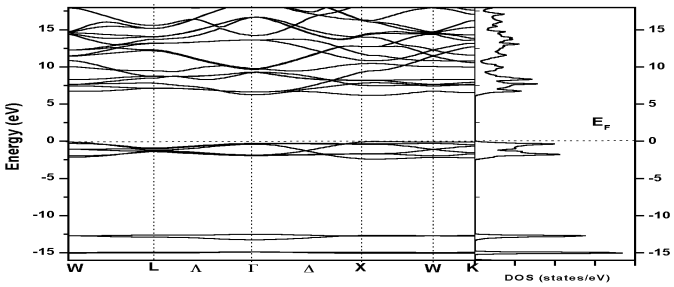

Fig. 2. Calculated band structure (left panel) and density of states (right panel) of $SrCl_2$ within EV-GGA approximation.

when the pressure is enhanced. To the best of our knowledge no experimental data or theoretical calculation for the pressure derivative of elastic constants for this compound has been reported yet. We believe that, our results can serve as a prediction for future investigations.

3.2 Electronic properties

Figure 2 (left panel), shows the calculated band structure at equilibrium volume within EV-GGA as a prototype since the band profiles are quite similar for both GGA and EV-GGA with a small difference in details. The results of our calculations using GGA show that the overall band profiles are in fairly good agreement with the FP-LMTO-GGA calculations [21] for the valence and conduction band configuration. Predicting the valence band maximum (VBM) at X point and conduction band minimum (CBM) at Γ point resulting in an indirect band gap. In the case of using EV-GGA, both VBM and CBM located at X point, indicating that $SrCl_2$ is a direct band gap material (X-X).

To further elucidate the nature of the electronic band structure, we have also calculated the density of states (DOS) as displayed in Figure 2 (right panel). Our results are consistent with those obtained by Kanchana et al. [21]. From the DOS we are able to identify the angular momentum character of the different structures. Following Figure 2, we should emphasize that there are four distinct structures in the density of electronic states separated by gaps. The lower bands (structures) contain Sr p states and Cl s states located at -15 eV and -12.75 eV below the Fermi level, respectively. The bandwidth of the upper valence band is about 2.5 eV, it is mainly derived from the Cl p sates. Looking at Figure 3, we notice that in the absence of the spin-orbit coupling there is a triple degeneracy at Γ point and a double degeneracy at X point. Including spin-orbit coupling in our calculations lifts the degeneracy at these points. The amount of the spin-orbit splitting is

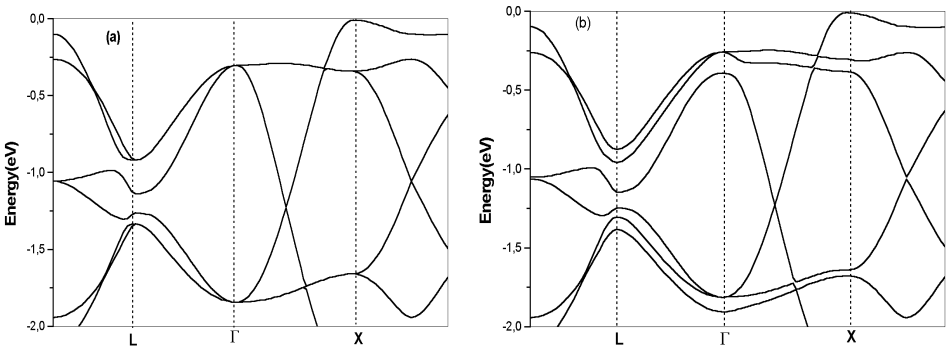

Fig. 3. The EV-GGA band structures (a) without SO coupling and (b) with SO coupling for energies close to the Fermi level.

Table 3. Calculated first- and second-order pressure coefficients of some direct and indirect band gaps (X-X, X-Γ, X-L, and Γ-Γ) and the upper valence band widths (UVBW) for $SrCl_2$. $E_g(P) = E_g(0) + \alpha P + \beta P^2$, E_g in eV, α in eV $\times 10^{-2}$ $(GPa)^{-1}$, β in eV $\times 10^{-4}$ $(GPa)^{-2}$.

	X-X	X-Γ	X-L	Γ-Γ	UVBW
GGA					
$E_g(0)$	5.53	5.25	6.71	5.52	2.62
α	1.16	10.07	2.02	11.55	
β	−2.77	−37.3	−10.5	−45.03	
Other study					
$E_g(0)^a$	5.55	5.18		5.54	2.75
Expt.^{b}		7.50			
EV-GGA					
$E_g(0)$	6.20	6.28	7.15	6.53	2.36
α	1.65	8.11	4.64	9.25	
β	−10.31	−40.63	−17.65	−45.43	

[a]Reference [21]; [b] reference [16].

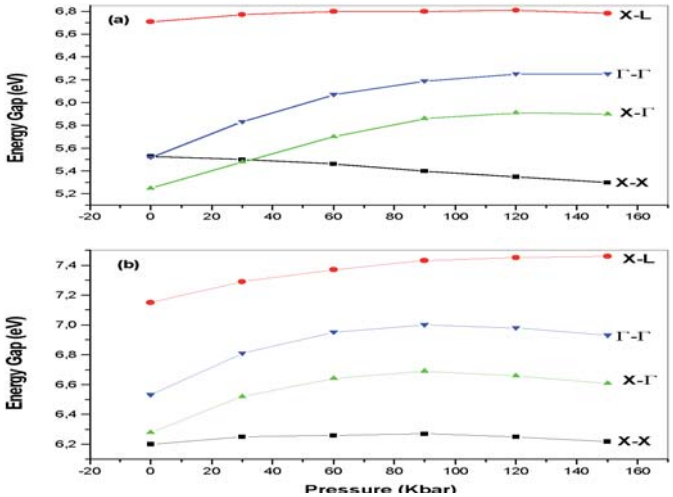

Fig. 4. Plots of the calculated band gaps versus pressure of SrCl2 with (a) GGA and, (b) EV-GGA.

0.15 eV and 0.1 eV at Γ and X points, respectively. The conduction bands are dominated by strontium d states, with a mixture of chloride d and strontium s states.

The calculated values of the band gaps and valence bandwidths for $SrCl_2$ compound within GGA and EV-GGA are listed in Table 3 along with experimental values and other previous theoretical calculations. It is clearly seen that the band gap obtained by GGA are lower than the experiment values and not far from the results obtained by the FP-LMTO method with the same exchange-correlation approximation. This underestimation of the band gap is mainly due to the fact that the simple form of GGA is not sufficiently flexible for accurately reproducing both exchange-correlation energy and its charge derivative. Engel and Vosko [30] constructed a new functional form of the GGA, namely EV-GGA, which proved to improve the results for quantities that depend on the energy eigenvalues, including the band gaps [31]. On the other hand, this approximation cannot give reliable bulk properties [12,31,45,46]. The values of calculated band gaps with EV-GGA show a significant improvement over the earlier results based on GGA compared to the experimental value.

In order to investigate the effects of the pressure on the size of the energy gaps of $SrCl_2$ compound in its cubic structure, the band energies at selected symmetry points are examined as a function of pressure. Figure 4 shows the plots of the pressure variations of the direct and indirect band gaps of $SrCl_2$ within GGA and EV-GGA. The calculated band gaps are well fitted to a quadratic function:

$$E_g(P) = E_g(0) + \alpha P + \beta P^2$$

where E_g is in eV, the pressure P is in GPa, α and β are the linear and quadratic pressure coefficients, respectively. The calculated values of α and β for the respective band gaps arising from X→X, X→ Γ, X→L and $\Gamma \rightarrow \Gamma$ transitions are also given in Table 3. Following Figure 4, we can notice a crossover between the indirect gap (X-Γ) and the direct gap (X-X) curves occurs at about 3.38 GPa, resulting in the energy minimum of direct gap for GGA. The indirect gap (X-L) increases with pressure for both GGA and EV-GGA. The direct gap (X-X) decreases linearly with pressure for GGA. While for EV-GGA the situation is a quite different where the direct gap (X-X) initially increases with the pressure up to 9.0 GPa and then decreases as a function of pressure. The direct (Γ-Γ) and indirect (X-Γ) band gaps exhibit the same type

of response to increase in pressure in both approximations with a strong sub-linear behaviors. Extremely large quadratic pressure coefficients are found compared to that of (X-X) and (X-L) band gaps. There is no experimental or theoretical result concerning the pressure dependence of band gaps is available.

3.3 Optical properties

The optical properties of matter can be described by mean of the transverse dielectric function $\varepsilon(\omega)$. There are two contribution to $\varepsilon(\omega)$, namely intraband and interband transitions. The contribution from intraband transitions is important only for metals. The interband transitions can further be split into direct and indirect transitions. Here we neglect the indirect interband transitions which involve scattering of phonon and are expressed to give only a small contributions to $\varepsilon(\omega)$ [47]. To calculate the direct interband contributions to the imaginary parts of the dielectric function$\varepsilon_2(\omega)$, one must sum up all possible transitions from the occupied to the unoccupied states. Taking the appropriate transition matrix elements into account, the imaginary part of the dielectric functions $\varepsilon_2(\omega)$ is given by :

$$\varepsilon_2(\omega) = \frac{Ve^2}{2\pi\hbar m^2\omega^2} \int d^3k \sum_{nn'} |\langle kn|p|kn'\rangle|^2 \, \mathrm{f}(kn) \times [1 - \mathrm{f}(kn')] \; \delta\left(\mathrm{E}_{kn} - \mathrm{E}_{kn'} - \hbar\omega\right) \quad (3)$$

where $\hbar\omega$ is the energy of the incident phonon, p is the momentum operator$\frac{\hbar}{i}\frac{\partial}{\partial x}$, $|kn\rangle$ is the eigenfunction with eigenvalue E_{kn}, and $f(kn)$ is the Fermi distribution function. The evaluation of the matrix elements of the momentum operator in equation (1) is performed over the muffin-tin and interstitial regions separately. A full detail description of the calculation of these matrix elements is given by Ambrosch-Draxl and Sofo [48].

The real part $\varepsilon_1(\omega)$ of the frequency dependent dielectric function can be derived from the imaginary part using the Kramers-Kronig relations. The knowledge of both real and imaginary parts of the frequency dependent dielectric function allows the calculations of important optical functions such as the refractive index $n(\omega)$, reflectivity $R(\omega)$ and absorption coefficient $I(\omega)$.

In the calculations of the optical properties, a dense mesh of uniformly distributed $\boldsymbol{k}$-points is required. Hence, the Brillouin zone integration was performed with 286 and 195 $\boldsymbol{k}$-points in the irreducible part of the Brillouin zone. We find very small differences between both calculations. In this paper we present the calculations with 195 $\boldsymbol{k}$-points. Broadening is taken to be 0.2 eV. Since, the EV-GGA seems to lead better band gaps rather than GGA, it was considered in our calculations of the optical properties based on the optimized structure models by GGA.

Figure 5 displays the variation of the imaginary (absorptive) part of the electronic dielectric function $\varepsilon_2(\omega)$ at ambient and less than 15.0 GPa pressure for a radiation up to 30 eV within only GGA-EV. Our analysis of the

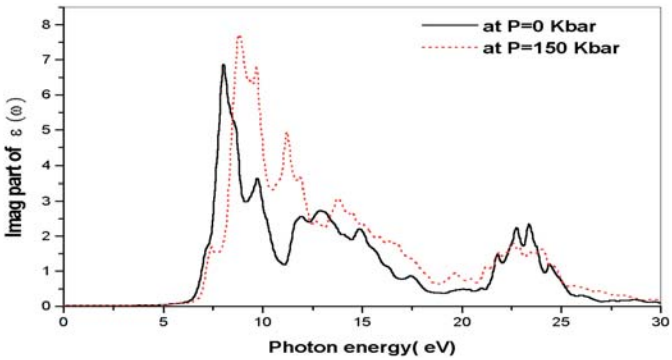

Fig. 5. Calculated imaginary part with and without pressure of the dielectric function of $SrCl_2$ with EV-GGA.

$\varepsilon_2(\omega)$ curve show that the threshold energy (first critical point) of the dielectric function occurs at 6.27 eV. This point is $X_v - X_c$ splitting which gives the threshold for direct optical transitions between the highest valence and the lowest conduction band. This is known as the fundamental absorption edge. Beyond these points, the curve increase rapidly. This is due to the fact that the number of points contributing towards $\varepsilon_2(\omega)$ increases abruptly.

The principle peak in the spectra is situated at 7.98 eV. This peak comes from direct transition at L point. This principle peak is followed by three other peaks localised at around 9.73 eV, 12.97 eV and 23 eV. Using our calculated band structure it would be worthwhile to identify the interband transitions that are responsible for the structure in $\varepsilon_2(\omega)$. The first structure can be assigned to direct transitions along the (L-Γ), Λ and Δ directions. The second one is primarily due to W-W transition with contributions of direct transitions along transitions X-W direction, while the last structure is coming from direct transition between bands situated at about -12 eV and conduction bands along Λ, Δ and W-L directions.

It is obvious that the chlorine $p$states and strontium d states play the major role in these optical transitions as initial and final states respectively. Spin-orbit coupling does not have any significant effect on the results. This is being expected, since the spin-orbit coupling changes the eignevalues only by around 0.1 eV, which is not significant in the calculations of the optical properties. This also has been found by previous FP-LAPW and FP-LMTO calculations for SrX, WSe_2 and HgI_2 [49–51].

When we compress this material, the positions of all critical points cited above are shifted towards higher energies. The reason lies on the enhancement of different gaps under pressure. Although the positions of these peaks are shifted under pressure but they are still of the same type as those at zero pressure. Moreover, the intensity of these main or global peaks is higher and sharper under pressure.

In Figure 6, we show the refractive index$n(\omega)$, reflectivity spectrum$R(\omega)$, and the absorption spectrum $I(\omega)$ for $SrCl_2$ at normal and high pressure. From Figure 6, we note that all spectra are shifted toward larger values. The static refractive index $n(0)$ is found to have the value 1.685 which is in good agreement with these obtained by

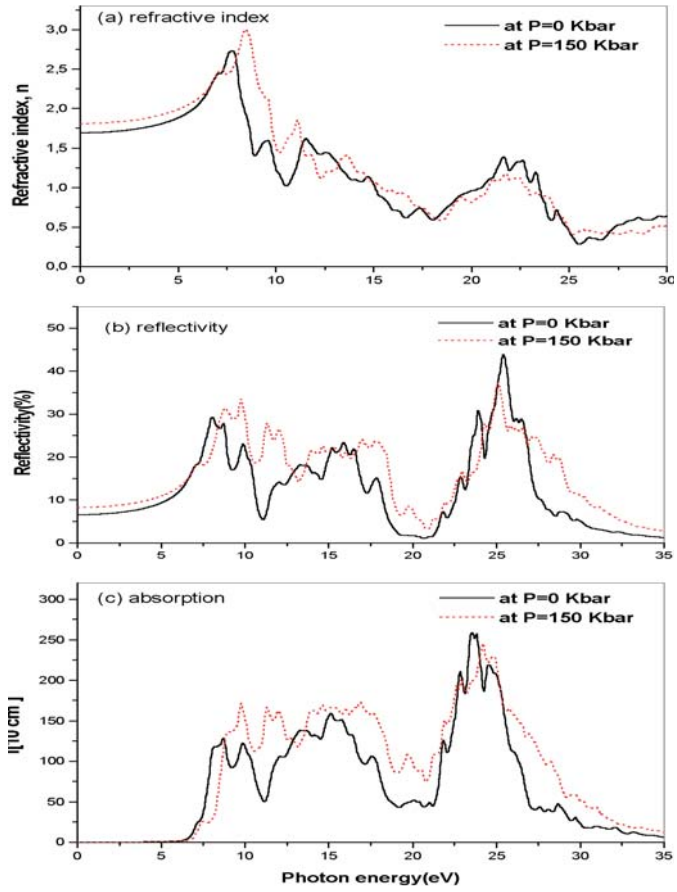

Fig. 6. Calculated refractive index $n\,(\omega)$, reflectivity $R\,(\omega)$ and absorption coefficient $I\,(\omega)$of SrCl2 with EV-GGA.

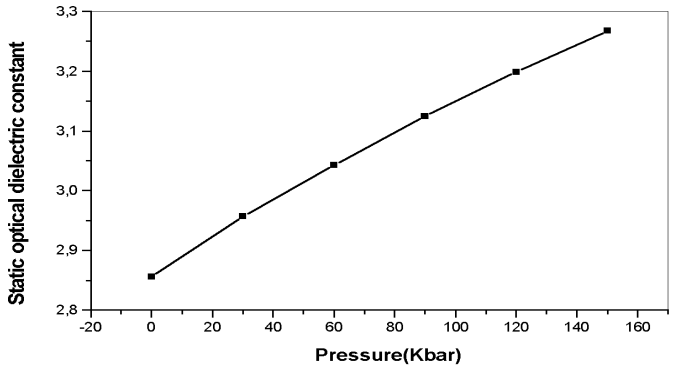

Fig. 7. Pressure dependence of ε_∞ of $SrCl_2$ with EV-GGA.

the goniometric apparatus measurements [52]. The refractive index reaches a maximum value of 2.7 at 7.8 eV. The reflectivity spectrum starts at around 7.0% and reaches the maximum value at about 30%. There is a dip in reflectivity spectra at around 20 eV, after that it is increases and reaches other maximum value.

The static dielectric constant $\varepsilon_1(0)$ is given by the low energy limit of $\varepsilon_1\,(\omega)$. Note that we do not include phonon contributions to the dielectric screening, and $\varepsilon_1(0)$ corresponds to the static optical dielectric constant ε_∞ . The calculated optical dielectric constant ε_∞ is 2.85. Figure 7 shows the calculated pressure dependence of the static optical dielectric constant. We note that the increase of the dielectric constants (refractive index) with pressure is practically linear for this compound. The pressure derivative of the refractive index $\boldsymbol{n}(\omega)$ of this compound is determined by a polynomial fit. Our calculated pressure, volume coefficients $\frac{1}{n_0}\frac{dn}{dp}$ and $\frac{v_0}{n_0}\frac{dn}{dv}$ are found to be equal 4.615×10^{-5} GPa^{-1} and -3.21, respectively. To the best of our knowledge, there is no experimental and theoretical result for the variation of the refractive indices under pressure for this compound.

4 Conclusions

This study reports a detailed investigation on the structural, electronic, elastic and optical properties of $SrCl_2$ compound using first principle FP-LAPW+lo method within LDA, GGA and EV-GGA. The most relevant conclusions are summarized as follows: (i) in comparison with the available experimental and theoretical results, the calculated GGA structural parameters and elastic constants are better than the LDA; (ii) our calculated band gaps, using GGA, are in good agreements with other computational works. In comparison with experiments, the calculated band gaps within EV-GGA show a significant improvement over the LDA and GGA results; (iii) the $SrCl_2$ compound is found to be a direct gap material with EV-GGA and an indirect gap (X-Γ) material by using the GGA; (iv) the spin-orbit coupling does not have any significant effect on the electronic and optical properties; (v) to the best of our knowledge, there are no earlier studies on the effect of pressure on the elastic constants, electronic structure and imaginary part of the dielectric constant, we feel that our calculations can be use to cover the lack of data of this compound.

The authors (A.B.) and (R.K.) wishes to acknowledge the help of Prof. Fouad El Haj Hassan (El-Hadath University-Libanon) and Doctor Rashid Ahmed (Punjab University Pakistan). For the author Ali Hussain Reshak this work was supported from the institutional research concept of the Institute of Physical Biology, UFB (No. MSM6007665808), and the Institute of System Biology and Ecology, ASCR (No. AVOZ60870520).

References

1. B. Welber, M. Cardona, C.K. Kim, S. Rodriguez, Phys. Rev. B **12**, 5729 (1975)
2. C.S. Menoni, H.D. Hochheimer, I.L. Spain, Phys. Rev. B **33**, 5896 (1986)
3. X. Zhu, S. Fahy, S.G. Louie, Phys. Rev. B **39**, 7842 (1989)
4. S.-H. Wei, A. Zunger, Phys. Rev. B **60**, 5404 (1999)
5. J.M. Leger, J. Haines, A. Atouf, Phys. Rev. B **51**, 3902 (1995)
6. M. Elaine, G. Tom, L. Kurt, J. Phys. Chem. Solids. **62**, 1117 (2001)

7. L.E. Nagel, M. O'Keeffe in *Fast Ion Transport in Solids*, edited by W. Van Gool (North Holland, Amsterdam, 1973), p. 165
8. J.M. Réau, P.P. Fedorov, L. Rabardel, S.F. Matar, P. Hagenmuller, Mater. Res. Bull. **18**, 1235 (1983)
9. X. Xu, T. Zhu, Hydrometallurgy **76**, 11 (2005)
10. R. Khenata, B. Daoudi, M. Sahnoun, H. Baltache, M. Rérat, A.H. Reshak, B. Bouhafs, H. Abid, M. Driz, Eur. Phys. J. B **47**, 63 (2005)
11. V. Kanchana, G. Vaitheeswaran, M. Rajagopalan, J. Alloy and Compounds **359**, 66 (2003)
12. X. Wu, S. Qin, Z. Wu, Phys. Rev. B **73**, 134103 (2007)
13. L.H. Brixner, Mater. Res. Bull. **11**, 1453 (1976)
14. B.M. Voronin, S.V. Volkov, J. Phys. Chem. Solids. **62**, 1349 (2001)
15. D.R. Jennison, A.B. Kunz, Phys. Rev. B **13**, 5597 (1976)
16. C. Sugiura, Phys. Rev. B **9**, 2679 (1974)
17. V. Tabakova, Solid State Commun. **87**, 135 (1993); V. Tabakova, Mater. Chem. Phys. **38**, 91 (1994)
18. Z. Pan, L. Ning, B.-M. Cheng, P.A. Tanner, Chem. Phys. Lett. **428**, 78 (2006)
19. J. Grimm, O.S. Wenger, K.W. Krämer, H.U. Güdel, J. Luminescence **126**, 590 (2007)
20. H.V. Lauer, K.A. Solbreg, D.H. Kühner, W.E. Bron, Phys. Lett. **35A**, 219 (1971)
21. V. Kanchana, G. Vaitheeswaran, A. Svane, J. Alloys and Compounds doi:10.1016/j.jallcom.2007.01.163 (in press)
22. S. Gao, Computer Physics Communications **153**, 190 (2003).
23. K. Schwarz, J. Solid State Chemistry **176**, 319 (2003)
24. R.W.G. Wyckoff, *Crystal Structures*, Vol. 1, 2nd edn. (Interscience Publishers, New York, 1982)
25. G.K.H. Madsen, P. Blaha, K. Schwarz, E. Sjöstedt, L. Nordström, Phys. Rev. B **64**, 195134 (2001)
26. K. Schwarz, P. Blaha, G.K.H. Madsen, Comput. Phys. Commun. **147**, 71 (2002)
27. P. Blaha, K. Schwarz, G.K.H. Madsen, D. Kvasnicka, J. Luitz, *WIEN2k, An augmented plane wave plus local orbitals program for calculating crystal properties*, Vienna University of Technology, Austria (2001)
28. J.P. Perdew, A. Zunger, Phys. Rev. B **23**, 5048 (1981)
29. J.P. Perdew, S. Burke, M. Ernzerhof, Phys. Rev. Lett. **77**, 3865 (1996)
30. E. Engel, S.H. Vosko, Phys. Rev. B **47**, 13164 (1993)
31. P. Dufek, P. Blaha, K. Schwarz, Phys. Rev. B **50**, 7279 (1994)
32. H.J. Monkhorst, J.D. Pack, Phys. Rev. B **13**, 5188 (1976)
33. F.D. Murnaghan, Prot . Natl. Acad. Sci. USA. **30**, 244 (1944)
34. F. El Haj Hassan, H. Akbarzadeh, S.J. Hashemifer, A. Mokhtari, J. Phys. Chem. Solids **65**, 1871 (2004)
35. F. El Haj Hassan, H. Akbarzadeh, S.J. Hashemifer, J. Phys.: Condens. Matter **16**, 3329 (2004)
36. M.J. Mehl, Phys. Rev. B **47**, 2493 (1993)
37. R. Khenata, M. Sahnoun, H. Baltache, M. Rérat, A.H. Reshak, Y. Al-Douri, B. Bouhafs, Phys. Lett. A **344**, 271 (2005)
38. R. Khenata, A. Bouhemadou, A.H. Reshak, R. Ahmed, B. Bouhafs, D. Rached, Y. Al-Douri, M. Rérat , Phys. Rev. B **75**, 195131 (2007)
39. R. Sahara, T. Shishido, A. Nomura, K. Kudou, S. Okada, V. Kumar, K. Nakajima, Y. Kawazoe, Comput. Mater. Sci. **36**, 12 (2006)
40. L. Kleinman, Phys. Rev. **128**, 2614 (1962)
41. M.B. Kanoun, A.E. Merad, J. Cibert, H. Aourag, G. Merad, J. Alloys Compounds **366**, 86 (2004)
42. A.E. Merad, H. Aourag, B. Khalifa, C. Mathieu, G. Merad, Superlatt. Microstruct. **30**, 241 (2001)
43. V. Kanchana, G. Vaitheeswaran, A. Svane, A. Delin, J. Phys. Condens. Matter **18**, 9615 (2006)
44. R. Dovesi, C. Roetti, C. Freyria-Fava, M. Prencipe, Chen. Phys. **156**, 11 (1991)
45. A. Mokhtari, H. Akbarzadeh, Physica B **337**, 122 (2003)
46. Z. Charifi, H. Baaziz, F. El Haj Hassen, N. Bouarissa, J. Phys. Condens. Matter **17**, 4083 (2005)
47. N.V. Smith, Phys. Rev. B **3**, 1971 (1862)
48. C. Ambrosch-Draxl, J.O. Sofo, Comput. Phys. Commun. **175**, 1 (2006)
49. R. Ahuja, O. Eriksson, B. Johansson, S. Auluck, J.M. Wills, Phys. Rev. B **54**, 10419 (1996)
50. S. Sharma, C. Ambrosch-Draxl, M.A. Khan, P. Blaha, S. Auluck, Phys. Rev. B **60**, 8610 (1999)
51. M. Dadsetani, A. Pourghazi, Phys. Rev. B **73**, 195102 (2006)
52. K. Shirao, Y. Fujii, J. Tominaga, K. Fukushima, Y. Iwadate, J. Alloys Compounds **339**, 309 (2002)